Control of Four-Level Quantum Coherence via Discrete Spectral Shaping of an Optical Frequency Comb

Matthew C. Stowe, Avi Pe'er, and Jun Ye

JILA, National Institute of Standards and Technology and University of Colorado
Department of Physics, University of Colorado, Boulder, Colorado 80309-0440, USA

(Received 30 January 2008; published 22 May 2008)

We present experiments demonstrating high-resolution and wide-bandwidth coherent control of a four-level atomic system in a diamond configuration. A femtosecond frequency comb is used to excite a specific pair of two-photon transitions in cold ^{87}Rb. The optical-phase-sensitive response of the closed-loop diamond system is studied by controlling the phase of the comb modes with a pulse shaper. Finally, the pulse shape is optimized resulting in a 256% increase in the two-photon transition rate by forcing constructive interference between the mode pairs detuned from an intermediate resonance.

DOI: 10.1103/PhysRevLett.100.203001 PACS numbers: 42.50.Gy, 32.30.−r, 32.80.Qk, 42.62.Eh

The field of coherent control of light-matter interactions for the purpose of driving a quantum system to a desired state has been drawing increasing interest. Research in the field of coherent control generally uses either an ultrashort pulse to create atomic coherences over a very large bandwidth, or in the other extreme, continuous wave (cw) lasers to drive transitions with high-resolution. Some of the pioneering work on coherent control used pulse shaping of a single broad-bandwidth pulse to enhance or diminish two-photon absorption [1,2], improve the resolution of coherent anti-Stokes Raman scattering [3], and control molecular wave packet motion [4]. A tremendous amount of research has also been done using narrow-bandwidth cw lasers to control three-level atomic systems, for example, to study electromagnetic induced transparency [5]. Relevant to this Letter are studies of closed-loop four-level systems, in either a double-Lambda [6] or diamond type configuration [7]. Experiments on closed-loop excitations have traditionally been conducted over a narrow ~10 GHz spectral range [8], restricted by the bandwidth of electro-optic modulators. This technique has been applied to phase correlation of independent lasers [9], proposed for amplification [10] and lasing without inversion [11], phase control of entanglement between coupled two-level systems [12], and control of molecular photodissociation pathways [13]. Optical frequency combs have made a strong impact on the field of high-precision spectroscopy [14], and have recently been used for coherent control of a three-level system [15]. In this work we combine the broad bandwidth and high resolution of the comb, augmented by spectral phase shaping, to vastly extend the bandwidth over which long-term quantum coherence is created and controlled.

We use a femtosecond optical frequency comb to excite a pair of resonant two-photon transitions that form a closed diamond configuration in cold ^{87}Rb; see Fig. 1(a). The broad bandwidth of the femtosecond pulses allows for a two-photon transition to be excited via different intermediate states with a separation of 7 THz. Simultaneously, the narrow linewidth of each comb mode allows the excitation of only specific atomic levels, a necessary condition to isolate the four-level diamond configuration from the full set of atomic transitions. The phase-sensitive excitation of this closed four-level system is demonstrated by discrete spectral shaping of the femtosecond comb. The 7 THz separation between intermediate states allows use of a pulse shaper to change the phase of the comb mode that is resonant with one intermediate state and not the other resonant modes, this shifts the relative phase between the two paths constituting the diamond. By analogy with an optical interferometer, the two-photon excitation is shown to exhibit a sinusoidal variation versus the applied phase.

The experiments presented in this Letter can be modeled as the interaction of an optical comb with arbitrary spectral phases and a four-level atomic system in a diamond configuration. There are hundreds of thousands of comb modes in the spectrum, four of which are tuned to be resonant with the transitions shown in Fig. 1(a). Because of the equidistant spacing of comb frequencies, any mode in the spectrum has another mode that forms a two-photon resonant pair. Therefore there are hundreds of thousands of

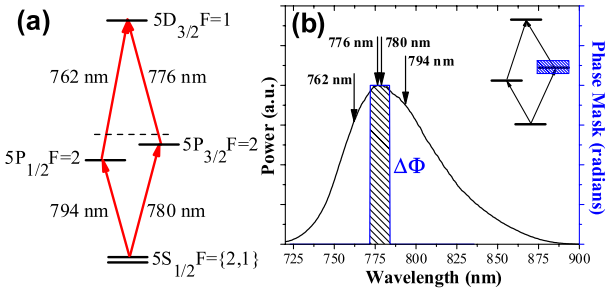

FIG. 1 (color online). (a) Energy level diagram of the diamond configuration in ^{87}Rb, the arrows indicate the resonant comb modes. (b) Pulse spectrum and phase mask used for the first experiment. The hatched region in the spectrum and the inset energy level diagram indicates the portion of the spectrum to which the phase mask is applied. The arrows indicate resonant wavelengths in relation to the phase mask.

mode pairs that are two-photon resonant but have varying detunings from the intermediate states; these will be referred to as off-resonant mode pairs. We present our experiments in two parts, the first focuses on the diamond configuration excited by resonant modes only, the second part utilizes another pulse shape to enhance the signal from the off-resonant mode pairs.

Resonant two-photon absorption via a pair of modes and one intermediate state results in an excited state amplitude that within second-order perturbation is,

$$c_{gf} \propto \frac{|E_n||E_m|e^{i(\phi_n+\phi_m)}\mu_{gi}\mu_{if}}{i(\omega_{gf} - (m+n)2\pi f_r - 4\pi f_o) + \gamma_f/2} \times \left[\frac{1}{i(\omega_{gi} - 2\pi(nf_r + f_o)) + \gamma_i/2} + \frac{1}{i(\omega_{gi} - 2\pi(mf_r + f_o)) + \gamma_i/2}\right], \quad (1)$$

where $|E_{n,m}|$ and $\phi_{n,m}$ are the electric field magnitudes and phases of the n^{th} and m^{th} comb modes, $\gamma_{i(f)}$ is the intermediate (final) state decay rate, $\omega_{gi(gf)}$ is ground to intermediate (final) state transition frequency, f_r is the repetition rate of the comb, f_o is the offset frequency, and $\mu_{gi(if)}$ are the dipole moments from the ground to intermediate (intermediate to final) states [16]. The total excited state amplitude is given by the sum of all the possible two-photon resonant transition pathways resulting from all comb mode pairs connecting through various intermediate states. The key physics for the results presented here is that the phase of the excited state amplitude is a function of the detuning from the intermediate state, the signs of dipole moment matrix elements, and the phase of the two electric fields. In particular, the phase of the excited state amplitude approaches $\pm 90°$ in the limiting case where the detuning of the considered comb mode is large compared to the intermediate state decay rate. Because of the phase difference of 180° between two excited state amplitudes symmetrically detuned about an intermediate resonance, the contribution to the total amplitude from the off-resonant mode pairs cancels to zero for transform-limited pulses. The four-mode configuration shown in Fig. 1(a) exhibits an optical phase dependence typical of closed-loop excitations. In the case of weak, resonant excitation with equal Rabi frequencies, the excited state population is proportional to $\cos(\frac{\psi}{2})^2$ with $\psi = \phi_{780} + \phi_{776} - \phi_{794} - \phi_{762}$, a characteristic feature of four-level closed-loop excitations [7].

The experiments are conducted on an ensemble of cold ^{87}Rb atoms formed in a magneto-optical trap (MOT). It is necessary to use cold atoms to ensure that only the four intended atomic states are excited, in contrast to a Doppler broadened room temperature gas. A Kerr lens mode-locked Ti:sapphire laser operating with an approximately 55 nm bandwidth centered at 778 nm with $f_r \approx 100$ MHz is used to excite all four transitions. f_r is phase stabilized to a low phase-noise crystal oscillator, and steered via a Cesium reference to maintain the absolute frequency of the comb modes. The offset frequency f_o is measured via a f-$2f$ nonlinear interferometer [17] and stabilized to a direct digital synthesizer. Regardless of the spectral phase of the pulses, any comb mode has an absolute frequency given by, $\nu_N = f_o + Nf_r$, where N is the mode order number (of order 10^6 for our laser). Using prior knowledge of the ^{87}Rb energy level structure for the $5S$, $5P$, and $5D$ hyperfine states, it is possible to select a particular f_r and f_o to approximate a diamond configuration with only four resonant levels [see Fig. 1(a)]. We use two values of f_r, the first is $f_r = 100.596\,606\,05$ MHz with $f_o = +16.94$ MHz. In this case, the four resonant states are: $5S_{1/2}F = 2$, $5P_{1/2}F = 2$, $5P_{3/2}F = 2$, and $5D_{3/2}F = 1$. With this selection of comb frequencies the transitions from $5S_{1/2}F = 1$, the other ground state, are at least 6 MHz detuned from any intermediate and excited states. All other possible transitions are further detuned. Note that the $5S$ to $5P$ and $5D$ linewidths are 6 and 0.66 MHz, respectively. Using a slightly shifted f_r of 100.596 605 25 MHz and the same f_o, the comb is resonant with the same intermediate and final states but from $5S_{1/2}F = 1$. We measure the $5D$ population by counting photons from the $5D$-$6P$-$5S$ cascade fluorescence at 420 nm. The experimental cycle consists of three parts: first a MOT is formed for 6.5 ms, then the atoms are held in optical molasses for 3 ms while the magnetic field turns off, finally, with cooling light off, the atoms are excited for 0.5 ms and the photon counts are recorded versus time on a multichannel scaler. We use a standard $2f$-$2f$ configuration pulse shaper with a computer controlled spatial light modulator (SLM) to set the phase of the comb modes with a pixel resolution of ~150 GHz [18]. The spatial and temporal frequency chirp of the pulses at the MOT location are reduced to maximize the fringe visibility.

The first experiment provides a clear demonstration of the phase-sensitive response of the four-level diamond configuration. We use the spatial light modulator to apply the phase mask in Fig. 1(b), the effect of which is to change the phase of all the mode pairs that are resonant from the ground state to $5D_{3/2}F = 1$ and close to the $5P_{3/2}$ intermediate states (denoted by the hatched region in Fig. 1(b)]. Specifically, the mask applies a variable phase step of Φ to the spectral region from 772 to 784 nm. Because of the aforementioned cancellation of the off-resonant amplitudes, it is sufficient to consider only the mode pairs tuned nearest to an intermediate state resonance here.

Our results are shown in Fig. 2, with each fringe fit to a function of the form, $\rho_{5D} = c_1 + c_2\cos(\Phi + c_3)^2$, where Φ is the phase applied to the SLM, c_3 is a static phase offset, and the visibility is given by $\frac{c_2}{2c_1+c_2}$. Because of the fact the phase mask covers both 780 nm and 776 nm, the two-photon amplitude from the resonant path through $5P_{3/2}F = 2$ is shifted by 2Φ and therefore has a period of π radians. The background counts due to ambient light at 420 nm and excitation of the hot Rb atoms not trapped in

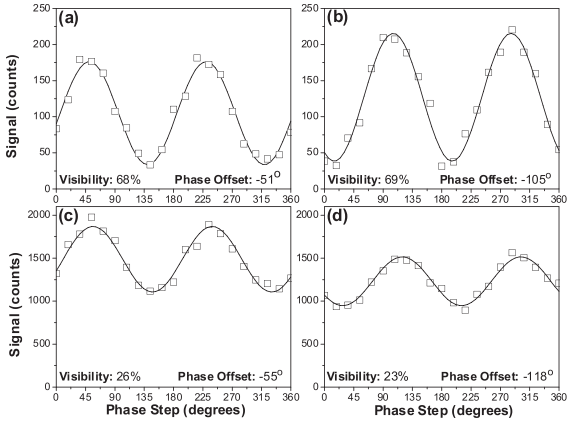

FIG. 2. (a) Measured interference fringes with fits under four different excitation conditions. All the results are obtained by scanning the phase Φ of the phase mask shown in Fig. 1(b). The top panels correspond to illuminating the atoms from only one direction (traveling waves). The bottom panels are under counter-propagating pulse excitation. The left panels (a) and (c) use the f_r for excitation from the $5S_{1/2}F = 2$ ground state; the right panels (b) and (d) use the f_r for excitation from the $5S_{1/2}F = 1$ ground state.

the MOT are measured by repeating the experiment without a MOT and subtracted from the reported data. As mentioned previously, we choose to conduct this experiment with two different values of f_r. The left panels in Fig. 2 are measured with f_r set for two-photon transitions from the $5S_{1/2}F = 2$ ground state. The right panels are with the second f_r, resonant from the $5S_{1/2}F = 1$ ground state. For each f_r, we also measure the interference fringe under excitation from a single pulse propagation direction (Fig. 2 top) and counterpropagating pulses (Fig. 2 bottom).

Two important features of our results are the fringe visibility and phase offset. The results presented in Fig. 2 show significant differences in both the fringe visibility and phase offset as a function of excitation scheme. We begin by discussing the offset of the fringe from $\Phi = 0$. Because of the large separation of wavelengths used in this experiment and the dispersion of the pulse shaper and general optics, any residual chirp of the pulse can cause an overall phase shift common to all measured fringes. However, not all fringes are shifted by the same amount; in particular, excitation from the two different ground states yields results significantly out of phase. To explain this relative phase shift we refer to Table I, in which the key parameters to estimate the fringe visibility and phase shift are tabulated. The first and most dominant effect is due to the sign of the dipole matrix elements; for transitions from $5S_{1/2}F = 2$ all the dipole moments are negative; however, for transitions from $5S_{1/2}F = 1$ there is sign difference between different two-photon paths. Table I gives the angular part of the dipole matrix elements, $\langle Lm_F F \parallel \hat{\mathbf{r}} \parallel L'm'_F F' \rangle$, denoted as μ'_{gi} and μ'_{if}. Clearly the sign of the dipole moments affect the closed-loop interference.

TABLE I. Left column is the intermediate state for each two-photon transition with a resonant or near-resonant comb mode. Across the top are the reduced dipole moments, the detuning of the nearest mode from the intermediate state, the relative magnitude of the two-photon amplitude, and the phase of the amplitude. The top section is for transitions from $5S_{1/2}F = 2$ and the bottom from $5S_{1/2}F = 1$.

$5S_{1/2}F = 2$

Intermediate	μ'_{gi}	μ'_{if}	Δ(MHz)	$\lvert c_{gf}\rvert$	θ
$5P_{3/2}F = 2,\ m_f = 1$	-0.17	-0.07	0.2	3.0	$-3.8°$
$5P_{1/2}F = 2,\ m_f = 1$	-0.17	-0.09	0.4	3.4	$-7.6°$
$5P_{1/2}F = 1,\ m_f = 1$	-0.29	-0.26	-11.5	4.3	75.4°

$5S_{1/2}F = 1$

Intermediate	μ'_{gi}	μ'_{if}	Δ(MHz)	$\lvert c_{gf}\rvert$	θ
$5P_{3/2}F = 2,\ m_f = 1$	0.29	-0.07	-2.6	3.9	$-139.1°$
$5P_{1/2}F = 2,\ m_f = 1$	-0.29	-0.09	-2.5	4.8	39.8°
$5P_{1/2}F = 1,\ m_f = 1$	0.17	-0.26	-14.4	2.1	$-101.8°$

It is also necessary to consider the phase shift of a particular two-photon amplitude due to the detuning from the relevant intermediate state. For this we include in Table I the path through the additional intermediate state $5P_{1/2}F = 1$, although the nearest comb mode is detuned, the dipole moment is sufficiently large to make its contribution significant. Because of the detuning of this transition path, there is a large phase shift of the corresponding amplitude. The effect of this additional path through $5P_{1/2}F = 1$ is to phase shift the total transition amplitude via $5P_{1/2}$ relative to the $5P_{3/2}$ amplitude, and thus the fringe shift. This occurs for two-photon transitions from both ground states. However, as can be seen from the dipole moments and amplitudes in Table I, the effect of the $5P_{1/2}F = 1$ state is less for the $5S_{1/2}F = 1$ ground state case. The difference in fringe shift between Figs. 2(a) and 2(b), corresponding to excitation from the two ground states, is 54°. This is in good agreement with the theoretically predicted value of 56°.

The second feature, the fringe visibility, is a result of the interference between the $5P_{1/2}$ and $5P_{3/2}$ paths in the diamond and any additional signal that raises the fringe minimum. Referring to the results in Fig. 2, the fringe visibility is strongly reduced under standing-wave excitation and exhibits little dependence on the particular ground state. In the case of traveling wave excitation, all the atoms in the MOT are excited by the same relative magnitude of electric fields. The visibility predicted using the amplitudes presented in Table I is 82% for excitation from the $5S_{1/2}F = 2$ ground state and 92% for the $5S_{1/2}F = 1$ ground state, assuming equal populations in the m_F sublevels. The best experimental results obtained for the visibility are about 70%, shown in Figs. 2(a) and 2(b). Residual frequency and spatial chirps have likely lowered the observed visibility from the ideal case. For traveling wave excitation the interference effect is observed for only the

first 50 μs of excitation after which the atoms are Doppler shifted completely off of resonance due to radiation pressure. The data presented in Fig. 2 are only the first 10 μs of excitation; longer excitation reduces the fringe visibility.

The effect of radiation pressure on the atoms is reduced by probing with counter-propagating pulses [14]. The bottom panels of Fig. 2 present the fringe measured using well overlapped counter-propagating beams of the same intensity. Although we measure a constant fringe visibility in this case for an extended time of 300 μs, the multimode standing wave generated by the counterpropagating pulses reduces the visibility to ~25%. This effect arises because the four main resonance frequencies have different wavelengths and thus different standing-wave periods, so the magnitudes of the four resonant electric fields vary spatially. For example, in some regions of the atom cloud the 780 nm field is maximum while the 794 nm field is minimum, so interference is not possible. Therefore a spatial average over the atom cloud, taking into account the standing waves, must be conducted. Using the amplitudes given in Table I, the visibility under standing-wave excitation is 36% and 44% from the $F = 2$ and $F = 1$ ground states, respectively.

The first experiment focuses entirely on those comb modes near an intermediate resonance. This is due to the fact that the vast majority of modes cancel out and thus make no net contribution to the two-photon amplitude. In the second experiment, we use f_r and f_o for two-photon transitions from the $5S_{1/2}F = 2$ ground state and apply the phase mask presented in Fig. 3(b). This phase mask forces constructive interference between the amplitudes due to the off-resonant mode pairs, increasing the total signal. Recall for every two-photon resonant mode pair detuned below an intermediate state, there is a pair detuned approximately equally above the state. For a transform-limited pulse train, these two pairs of modes give rise to excited state amplitudes that are equal and opposite, and therefore cancel to zero. By applying the phase mask in Fig. 3(b), those modes that are detuned below either the $5P_{3/2}$ or $5P_{1/2}$ states [the hatched area in Fig. 3(b)] obtain a 180° phase shift with respect to those detuned above the intermediate state. This type of spectral phase negates the inherent phase change due to the detuning around a resonance [see Eq. (1)], and causes constructive interference. Figure 3(a) shows we achieve a maximum increase of 2.56 over the normal signal. The theoretical enhancement is 2.85; however, this estimate does not include the effects of diffraction at the phase steps in the SLM, which likely reduces the maximum. The data are obtained by first coarsely tuning the position of the phase mask at the per pixel resolution. Then for finer control of the location of the phase step applied to the comb spectrum, the entire SLM is shifted using a micrometer through the spectrally dispersed optical field.

We have demonstrated the precise control of a diamond configuration four-level atomic coherence over a 32 nm spectral width. The first experiment focuses on the comb modes resonant with intermediate states, and the second optimizes the two-photon transition rate using high-resolution spectral phase shaping to force constructive interference between the off-resonant modes. The unique capability of optical frequency combs combined with pulse shaping techniques to control long-term atomic coherences over a very broad-bandwidth opens up new experimental possibilities. For example, a technique to create deeply bound ultracold molecules by controlling two-photon transitions with many intermediate states excited by a comb has recently been proposed [19].

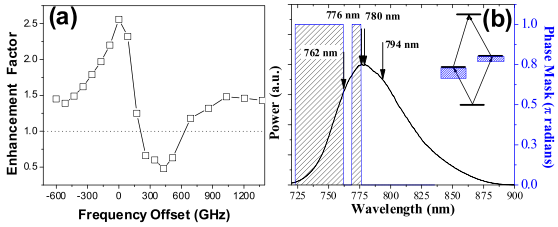

FIG. 3 (color online). (a) Measured signal enhancement. The ratio of signals with and without the phase mask in (b), versus position of the SLM in the spectrum. The zero of the offset frequency is chosen to be the position of the maximum signal increase. (b) The applied phase mask is indicated by the hatched region. Exactly π radians of phase is applied just below 762 and 776 nm to add an extra phase shift to those mode pairs that join in the hatched region.

We thank NSF, NIST, and DARPA for funding support.

[1] P. Balling, D. J. Maas, and L. D. Noordam, Phys. Rev. A **50**, 4276 (1994).
[2] N. Dudovich *et al.*, Phys. Rev. Lett. **86**, 47 (2001).
[3] D. Oron *et al.*, Phys. Rev. Lett. **88**, 063004 (2002).
[4] W. Salzmann *et al.*, Phys. Rev. A **73**, 023414 (2006).
[5] M. Fleischhauer, A. Imamoglu, and J. P. Marangos, Rev. Mod. Phys. **77**, 633 (2005).
[6] E. A. Korsunsky and D. V. Kosachiov, Phys. Rev. A **60**, 4996 (1999).
[7] G. Morigi, S. Franke-Arnold, and G.-L. Oppo, Phys. Rev. A **66**, 053409 (2002).
[8] W. Maichen *et al.*, Phys. Rev. A **53**, 3444 (1996).
[9] A. F. Huss *et al.*, Phys. Rev. Lett. **93**, 223601 (2004).
[10] O. Kocharovskaya and P. Mandel, Phys. Rev. A **42**, 523 (1990).
[11] E. S. Fry *et al.*, Opt. Commun. **179**, 499 (2000).
[12] V. S. Malinovsky and I. R. Sola, Phys. Rev. Lett. **93**, 190502 (2004).
[13] Z. Chen, P. Brumer, and M. Shapiro, J. Chem. Phys. **98**, 6843 (1993).
[14] M. C. Stowe *et al.*, Adv. At. Mol. Opt. Phys. **55**, 1 (2008); A. Marian *et al.*, Science **306**, 2063 (2004).
[15] M. C. Stowe *et al.*, Phys. Rev. Lett. **96**, 153001 (2006).
[16] T. H. Yoon *et al.*, Phys. Rev. A **63**, 011402(R) (2000).
[17] S. T. Cundiff and J. Ye, Rev. Mod. Phys. **75**, 325 (2003).
[18] A. M. Weiner, Rev. Sci. Instrum. **71**, 1929 (2000).
[19] A. Pe'er *et al.*, Phys. Rev. Lett. **98**, 113004 (2007).